chemosensors

MDPI

Communication

High-Performance Screen-Printed Triboelectric Nanogenerator Based on $BaTiO_3$-Enhanced Copy Paper for Sustainable Energy Harvesting

Omkar A. Patil [1], Jun Young Cheong [2], Baoyang Lu [3], Byungil Hwang [4,*] and Sooman Lim [1,*]

[1] Department of Flexible and Printable Electronics, LANL-JBNU Engineering Institute, Jeonbuk National University, Jeonju 54896, Republic of Korea; omkar1800@jbnu.ac.kr
[2] James Watt School of Engineering, University of Glasgow, Glasgow G12 8QQ, UK; junyoung.cheong@glasgow.ac.uk
[3] Jiangxi Province Key Laboratory of Flexible Electronics, Jiangxi Science & Technology Normal University, Nanchang 330013, China; luby@jxstnu.edu.cn
[4] School of Integrative Engineering, Chung-Ang University, Seoul 06974, Republic of Korea
* Correspondence: bihwang@cau.ac.kr (B.H.); smlim@jbnu.ac.kr (S.L.)

Abstract: This study investigates the triboelectric performance of nanogenerators based on copy paper (CP) and barium titanate (BTO) with varying concentrations (0%, 5%, 10%, 15%, and 20%). BTO was coated onto the paper surface via screen-printing, significantly enhancing the triboelectric properties. Results showed that as the BTO concentration increased, the output performance improved, with optimal performance observed at 15% BTO. At this concentration, the nanogenerator produced an output of 103 V and 3.6 μA. The CP/BTO nanogenerator demonstrated stable performance over 57,600 cycles at 4 Hz frequency and 40 N applied force, indicating excellent durability. The device attained a maximum power density of 32.4 μWcm^2, highlighting the efficiency improvement through BTO integration. Various parameters including BTO concentration, applied force, and frequency were studied to optimize device performance. The CP/BTO device successfully powered 60 LEDs and a calculator, demonstrating its potential for practical energy harvesting applications. This research presents a promising approach for developing low-cost, environmentally friendly power-generating systems for wearable and portable devices.

Keywords: barium titanate; copy paper; triboelectric nanogenerator; screen printing

check for updates

Received: 7 January 2025
Revised: 16 February 2025
Accepted: 17 February 2025
Published: 19 February 2025

Citation: Patil, O.A.; Cheong, J.Y.; Lu, B.; Hwang, B.; Lim, S. High-Performance Screen-Printed Triboelectric Nanogenerator Based on $BaTiO_3$-Enhanced Copy Paper for Sustainable Energy Harvesting. *Chemosensors* **2025**, *13*, 76. https://doi.org/10.3390/chemosensors13020076

Copyright: © 2025 by the authors. Licensee MDPI, Basel, Switzerland. This article is an open access article distributed under the terms and conditions of the Creative Commons Attribution (CC BY) license (https://creativecommons.org/licenses/by/4.0/).

1. Introduction

Triboelectric nanogenerators (TENGs) have emerged as a promising energy-harvesting technology due to their low-cost [1,2], excellent durability [3], and ease of processing [4]. While TENGs have been developed using various substrates such as silicone rubber [5], cotton [6], and silk [7], paper-based TENGs have garnered particular interest due to their unique advantages [8]. Copy paper (CP) offers a flexible [9], lightweight [10], cost-effective [11], and biocompatible substrate material [12], with distinct benefits compared to metal, acrylic, glass, and plastic. However, despite these advantages, paper-based TENGs have faced challenges in achieving high energy conversion efficiency [8–11]. The inherent limitations of paper's triboelectric properties have restricted the power output of these devices, hindering their practical applications in wearable electronics [13], electronic skin [14], and implantable medical devices [15]. TENGs have the capacity to scavenge energy from low-frequency mechanical vibrations [16], which are common in both natural and human-made surroundings. TENGs can be fabricated utilizing a wide range of materials, including

polymers, metals, and composite structures, providing flexibility in design and adaptation for various applications.

Electronic devices require precise fabrication techniques. The screen-printing technique is the most popular technique to develop electronic devices. One of the key benefits of screen printing is its capacity to create homogeneous and high-resolution patterns over huge areas [17], making it ideal for scaled manufacturing. TENGs enable the precise deposition of materials such as conductive inks, polymers, and nanomaterials onto flexible substrates, enabling for the integration of numerous layers that enhance energy conversion efficiency [18–20]. The screen-printing technique is a well-established and versatile fabrication method, particularly in the development of electronic devices such as triboelectric nanogenerators (TENGs). This process involves the deposition of materials, including conductive inks, polymers, and nanomaterials, onto a substrate through a mesh screen. It is highly valued for its ability to create precise, homogeneous, and high-resolution patterns over large areas, making it particularly suitable for scalable manufacturing. One of the key advantages of screen printing is its compatibility with flexible substrates, which allows for the deposition of multiple layers. This multi-layer capability is crucial for enhancing energy conversion efficiency in TENGs, as it provides better control over material distribution and device structure. Moreover, screen printing is cost-effective, fast, and well-suited for mass production [21,22].

Several materials have been widely reported in the development of triboelectric nanogenerators (TENGs), including metal oxides, 2D chalcogenides, metal–organic frameworks (MOFs), covalent organic frameworks (COFs), biopolymers, and biomaterials [23–25]. Ceramic materials have also been extensively explored in TENGs due to their promising properties. Ceramic materials, such as metal oxides and ferroelectrics, offer significant advantages in terms of triboelectric performance, durability, and stability. These materials are highly effective in converting mechanical energy into electrical energy through the triboelectric effect. Their ability to maintain performance over long cycles of contact and separation, coupled with their favorable electrical properties, makes ceramics an essential component in advancing the efficiency of nanogenerators stable [26,27]. Barium titanate (BTO) has been recognized as a highly effective material for enhancing triboelectric efficiency due to its excellent ferroelectric and dielectric properties [28–30]. Its perovskite structure allows for high spontaneous efficiency [31–33], making it a promising candidate for improving TENG's performance [34,35]. BTO is a very effective material for collecting mechanical energy from environmental sources including vibrations, human motion, and fluid movement due to its dual functionality [36]. While BTO has shown potential in various TENG applications [37,38], paper-based TENGs have limited durability, making them prone to damage from bending. Their low charge retention reduces efficiency and weakens performance. Surface modifications are challenging, restricting potential enhancements. Additionally, complex or non-scalable fabrication methods hinder large-scale applications. BTO integration with copy paper for TENGs has not been previously explored, presenting a novel opportunity for enhancing paper-based TENG performance [39,40].

In this study, we address the limitations of paper-based TENGs by investigating, for the first time, the integration of BTO onto the copy paper surface via screen-printing. Our work focuses on fabricating a copy paper-based TENG and systematically investigating the impact of screen-printed BTO on its performance. By depositing various concentrations of BTO (0% to 20%) onto the paper, we analyze how different levels of BTO influence the energy harvesting efficiency of the TENG. Our systematic study of various BTO concentrations revealed that the optimal performance was achieved with 15% BTO, producing an output of 103 V and 3.6 μA. The CP/BTO nanogenerator demonstrated remarkable durability, maintaining stable performance over 57,600 cycles at 4 Hz frequency and 40 N

applied force. We achieved a maximum power density of 32.4 μW/cm^2, significantly improving the energy harvesting efficiency compared to conventional paper-based TENGs. Furthermore, our CP/BTO device successfully powered 60 LEDs, demonstrating its practical applicability for energy harvesting. This study not only overcomes the limitations of previous paper-based TENGs but also presents a novel, efficient, and environmentally friendly approach to energy harvesting, leveraging the inherent advantages of paper-based devices while significantly enhancing their performance through BTO integration.

2. Materials and Methods

2.1. Materials

Barium titanate (BTO) nanoparticles, with an average particle diameter of 100 nm, US Research Nanomaterials Inc., Houston, TX, USA. Polytetrafluoroethylene (PTFE) thin sheet (0.08 mm thick), N-Methyl-2-pyrrolidone (NMP), Polyethene terephthalate (PET), and both conductive adhesive copper and aluminum were purchased from Sigma-Aldrich, (Seoul, Republic of Korea).

2.2. Screen-Print of the Film

The various percentages of barium titanate (BTO) nanoparticles (0% to 20%) were added in N-Methylpyrrolidone (NMP) 0.5 mL and crushed in a mortal pestle to obtain screen printable ink. The screen-printing technique was performed utilizing a screen printer (AMX-1242T Semi-Auto screen printer, Bucheon, Republic of Korea) with an emulsion screen mesh (325 mesh count, thread per inch, 830 μm opening, 39 μm mesh thickness) the screen-printed film dried in a vacuum oven at 60 °C for 24 h. Figure 1a depicts a schematic diagram of screen printing.

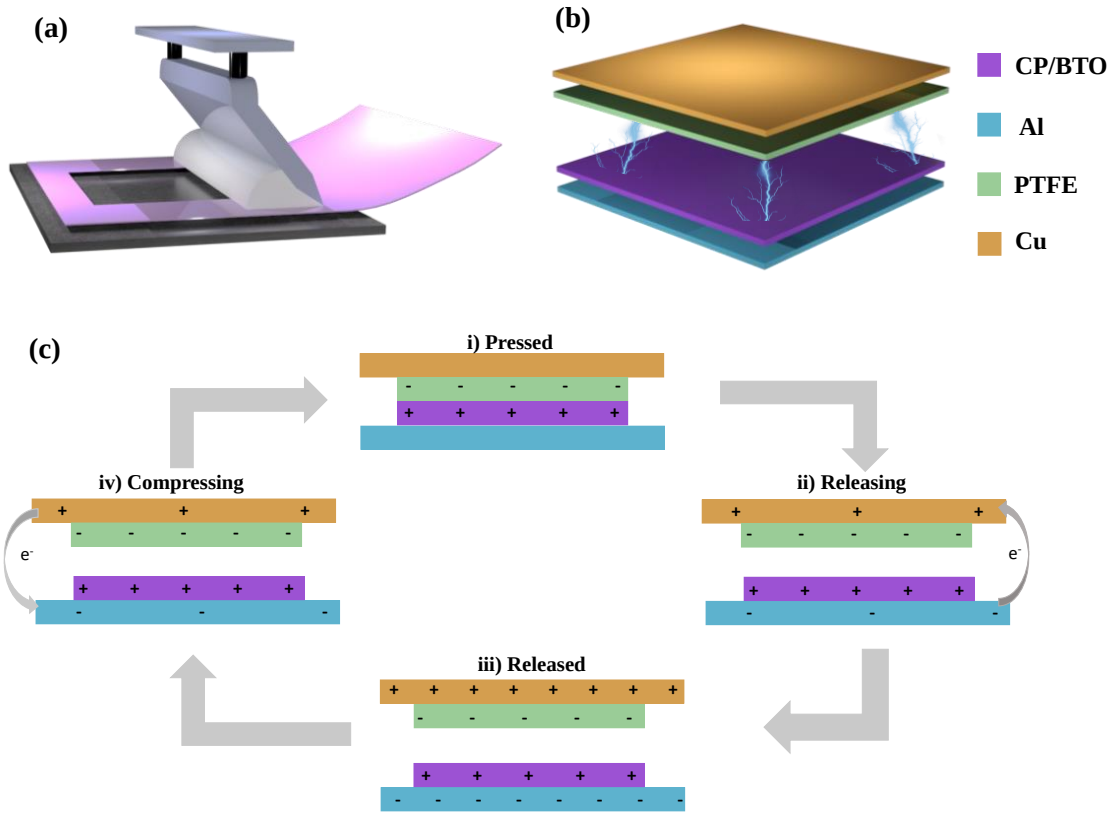


Figure 1. (**a**) Schematic diagram of Screen-printing. (**b**) Developed TENG structure (**c**) Schematic of the working mechanism of contact separation based on proposed TENG.

2.3. Device Fabrication of the TENG

In this proposed work, we have developed a vertical contact separation-based triboelectric nanogenerator. The triboelectric layers consist of two distinct materials: a tribopositive layer made from a barium titanate coated onto the surface of the copy paper (CP/BTO). The BTO material adhered to the paper through bonding, and the interaction between the BTO layer and the paper fibers helped ensure the film's stability without any peeling, and a tribonegative layer composed of polytetrafluoroethylene (PTFE). The CP/BTO film is adhered to a conductive adhesive aluminum foil, while the PTFE film is attached to a conductive adhesive copper foil. The flexible PET substrate was used as the supporting substrate which helps to easily form the contact separation method. The structure of the developed triboelectric nanogenerator is depicted in Figure 1b, showcasing the arrangement of the triboelectric layers.

2.4. Characterization

The printed samples of the chemical structure were studied using Fourier-transform infrared (FTIR) spectroscopy (Bomen MB 100, Bomen, Québec City, QC, Canada) in the wavenumber range of 400–4000 cm^{-1}. The printed sample morphologies were analyzed at the Jeonbuk National University Center for University-wide Research Facilities (CURF, Jeonju, Republic of Korea) using field emission scanning electron microscopy (FESEM, SUPRA 40VP, Carl Zeiss, Germany). The screen-printed TENGs output voltages and currents were measured using an oscilloscope (KEYSIGHT DSOX2012A, Santa Rosa, CA, USA) and a (Keithley 2450 source meter, Solon, OH, USA).

3. Results and Discussion

In this study, barium titanate oxide (BTO) and copy paper (CP) were used as tribo-positive materials, while PTFE served as the tribo-negative material. The triboelectric performance of the device was primarily governed by the charge transfer between the PTFE and CP/BTO layers upon the application of vertical force. PTFE, with its strong electronegativity, readily accepts electrons, while BTO and CP, exhibiting tribo-positive properties, donate electrons to the PTFE layer. As illustrated in (Figure 1c, (i)), when force is applied, the PTFE layer comes into contact with the CP/BTO layers, leading to electron transfer.

In addition to the conventional triboelectric interaction, we propose an enhanced mechanism involving ion exchange at the interface between the PTFE and CP/BTO layers. This ion exchange process, as described in previous studies [41,42], suggests that ionic species from the CP/BTO layers migrate to the interface with PTFE during contact. The migration of these ions contributes to the formation of localized ionic bonds at the interface, which strengthens the charge transfer and may increase the efficiency of the device. This ionic interaction effectively boosts the overall triboelectric performance by enhancing the charge density at the interface.

Upon removal of the applied force, as shown in (Figure 1c, (ii)), electrons and ions migrate toward the electrode, generating a voltage. When the force is completely removed, a large number of electrons and ions flow into the electronic circuit, generating a positive voltage (Figure 1c, (iii)). Reapplying the force reverses the movement of electrons and ions, leading to a negative output (Figure 1c, (iv)).

Fourier Transform Infrared (FTIR) spectroscopy of the printed CP/BTO is depicted in Figure 2a, exhibiting characteristic absorption bands. The pattern observed at 3000–3500 cm^{-1} is attributed to N-H stretching. The peaks observed at 1656 cm^{-1} are attributed to C=O stretching, while those at 1427 cm^{-1} correspond to either C-H bending or carbonate stretching [43]. The triboelectric nanogenerator operates based on the phe-

nomenon of surface charge generation, making the surface characteristics of the triboelectric layer a key factor in achieving higher output. Figure 2b shows the surface morphology of screen-printed BTO on the copy paper. The image reveals that the nanoparticles are effectively printed and evenly distributed across the copy paper. The hierarchical arrangement of the particles on the thin film is a critical factor in enhancing the performance of TENGs [44,45]. This is because the TENG's functionality relies on the contact and separation between the two triboelectric layers. Therefore, the distribution pattern of the BTO particles on the paper directly influences the electrical performance of the developed TENG. This arrangement ensures a more efficient charge transfer and enhances the overall performance of the triboelectric nanogenerator [46]. Additionally, a cross-sectional image of the BTO thin film is shown in (Supporting Information Figure S1a). Figure 2c depicts the EDX measurements of the CP/BTO thin film. The EDS spectrum of the thin film shows the presence of barium, titanium, and oxygen, which correspond to the BTO, as well as oxygen and carbon, which are associated with the copy paper. The elemental atomic composition of Ba, Ti, O, and C is 63.80%, 20.34%, 8.06%, and 8.22%, respectively. Figure 2d presents an elemental analysis of the CP/BTO thin film, suggesting that all the elements are evenly distributed within the film. The elemental mapping images of Ba, Ti, O, and C, shown in Figure 2e–h, indicate that these elements are well distributed across the thin film.

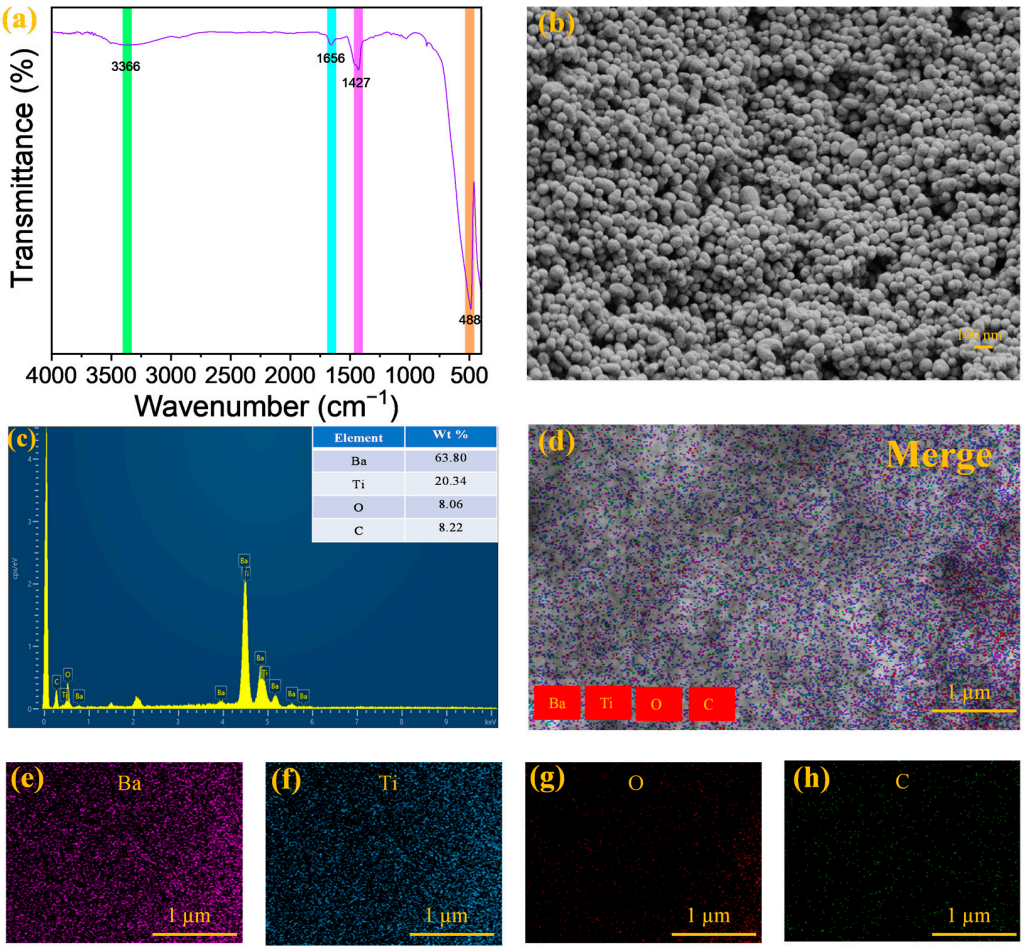


Figure 2. (**a**) FTIR of the CP/BTO. (**b**) FE-SEM image of the Screen printed BTO nano powder (**c**) EDX analysis of CP/BTO film. (**d**) Marge series OF BTO film. (**e**) Ba series. (**f**) Ti series (**g**) O series. (**h**) C series.

Figure 3 shows the output voltage and current of the device, where we studied several parameters such as various concentrations of CP/BTO materials and different

electronegative layers. We developed four tribopositive layers with varying amounts of BTO in the copy paper: 5%, 10%, 15%, and 20%. As shown in Figure 3a,b, the performance of the triboelectric nanogenerator increased as the BTO concentration increased from 5% to 20%. The bare copy paper generated 40 V and 1.1 μA, 5% BTO generated 62 V and 2.1 μA, 10% BTO generated 84 V and 2.7 μA, 15% BTO generated 103 V and 3.6 μA, and 20% BTO generated 90 V and 3.1 μA. These results suggest that CP/BTO is a promising candidate for developing efficient triboelectric nanogenerators. The increase in performance with BTO concentration can be attributed to the enhanced dielectric properties of BTO, which facilitate greater charge accumulation and separation during the contact–separation cycles. The BTO material layer significantly enhances the paper's ability to withstand high mechanical pressure, providing greater durability and stability. However, at 20% BTO, performance was slightly decreased, due to excessive BTO concentration impacting the material's durability and stability. The performance of the triboelectric nanogenerator depends not only on the tribopositive materials but also on the tribonegative material. In Figure 3c,d, we compared two electronegative layers: PET and PTFE. The CP/BTO with PET device generated 87 V and 2.5 μA, while the CP/BTO with PTFE produced 103 V and 3.6 μA. The CP/BTO with PTFE device generated a higher output due to the greater potential difference between the tribopositive and tribonegative layers. Additionally, fluorinated materials like PTFE possess higher tribonegativity, resulting in a more significant charge transfer during the interaction [47]. This highlights the importance of selecting the appropriate triboelectric pairs to maximize the performance of TENGs. The combination of optimal CP/BTO concentration with appropriate tribonegative materials like PTFE can significantly enhance the energy output of the device, making it a highly efficient triboelectric nanogenerator.

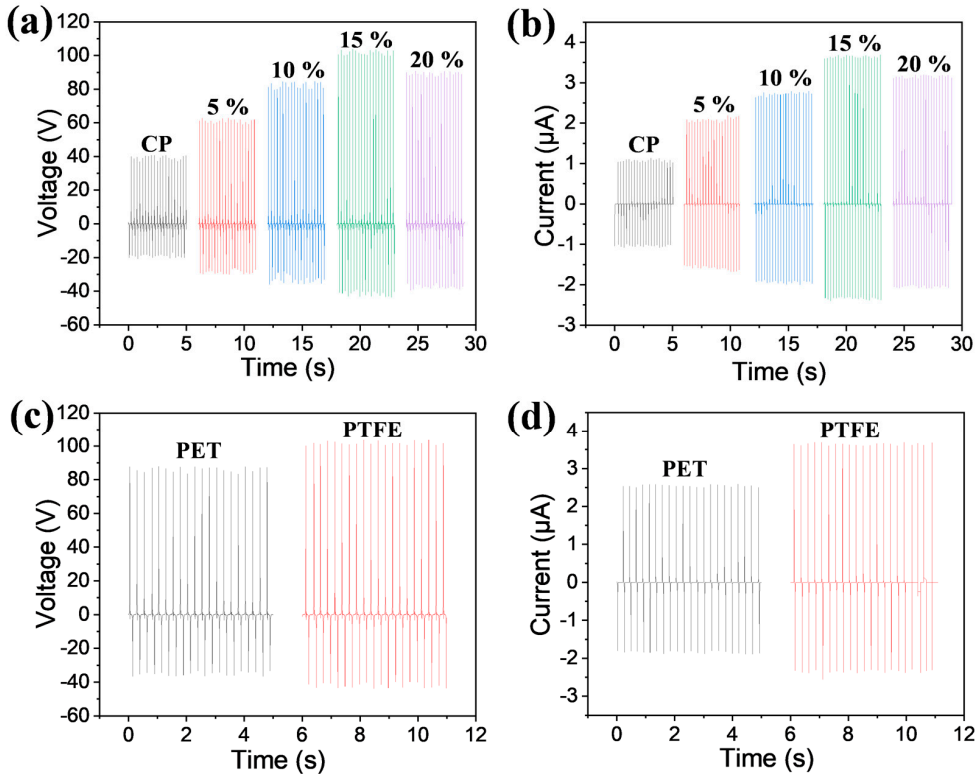


Figure 3. (**a**) Open-circuit voltage, (**b**) short-circuit current with different concentrations of BTO. (**c**) Open-circuit voltage, (**d**) short-circuit current with different electronegative layers.

Furthermore, in Figure 4a,b, we studied the effect of applied force on the device. As the triboelectric nanogenerator is a mechanical pressure-dependent device, pressure significantly impacts TENG performance. We applied three different forces (20 N, 30 N,

and 40 N) to the device, which demonstrated that the output increased with increasing pressure. The device generated 72 V and 2.2 μA at 20 N applied force, 83 V at 30 N, and 103 V and 3.6 μA at 40 N, which was higher than the previous voltages. This increase can be attributed to the enhanced contact area and formation between the triboelectric layers under higher forces, resulting in more efficient charge transfer during the contact separation cycle. While force is a crucial characteristic in developing high-performance TENGs, frequency is equally important because the separation rate of the device also impacts performance [48]. In Figure 4c,d, we studied three frequencies applied to the device. Initially, at 2 Hz, the device generated 65 V and 1.8 μA. At 3 Hz, it produced 85 V and 2.6 μA, and at 4 Hz, it reached 103 V and 3.6 μA, this behavior indicates a frequency-dependent charge accumulation process, where higher frequencies enhance the rate of charge generation and transport due to more rapid separation of the triboelectric layers. after which the output began to saturate. Furthermore, we studied the output voltage of different thickness of BTO shows in the (Supporting Information Figure S1b). These results suggest that the separation rate is a critical parameter in developing efficient triboelectric nanogenerators.

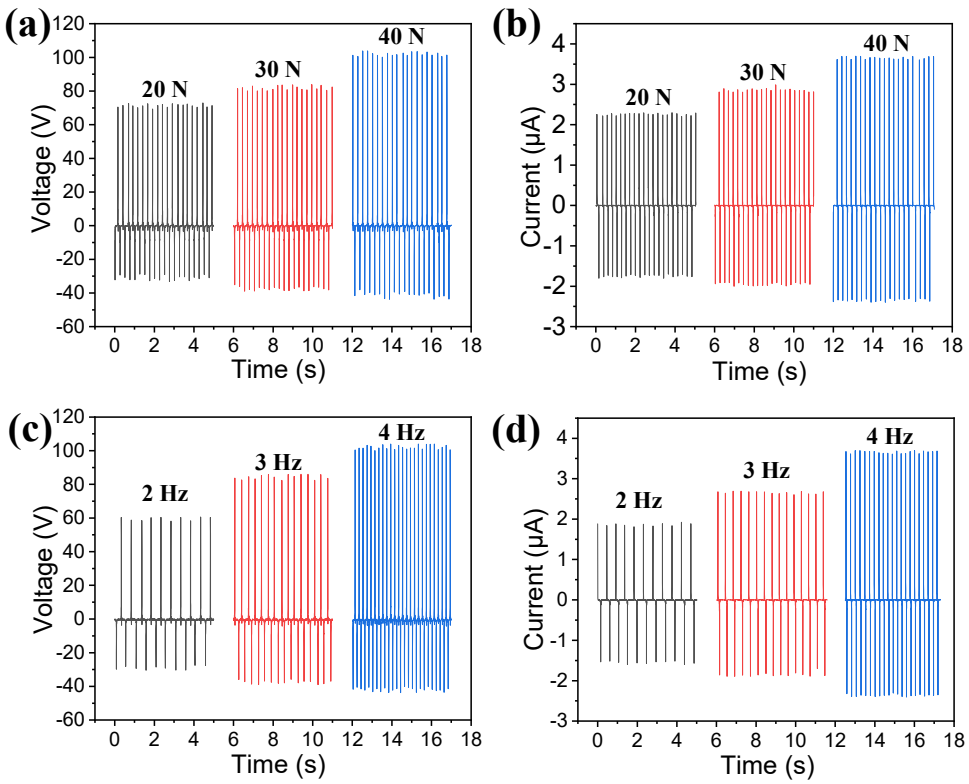


Figure 4. Output (**a**) voltage and (**b**) current by applying different force of CP/BTO TENG. Output (**c**) voltage and (**d**) current by applying various frequencies.

Figure 5a illustrates the CP/BTO device stability during continuous operation at a frequency of 4 Hz and an applied force of 40 N over a 57,600-cycle period. Notably, no performance or structural degradation was observed, demonstrating the device's endurance, and indicating the device's long-term durability and mechanical robustness. This result is significant as it underscores the reliability of the CP/BTO TENG's durability for long-term usage in energy harvesting applications requiring operational stability. Figure 5b shows the output power of the device as the resistance varies from 100 Ω to 100 MΩ. The current of the device decreases as the load resistance increases. However, the power of the device initially increases from 100 Ω to 10 MΩ, after which it starts to decrease. The proposed device shows the highest power density at 10 MΩ, which is 32.4 $\mu W/cm^2$. The optimized

CP/BTO composition and device design helped to increase charge transfer and energy conversion efficiency. Moreover, the real-time applicability of the device was studied through the charging of various capacitors, as shown in Figure 5c. Since the nanogenerator produces AC output while the capacitors require DC input, we used a bridge rectifier to convert the AC signals into DC. The device successfully charged 1 µF, 4.7 µF, and 10 µF capacitors. The screen-printed device's output performance enables the powering of low-power electronic devices without the need for an intermediary energy storage system. Figure 5d. depicts the entire circuitry for LED lighting, including a bridge rectifier as an essential supporting component. To investigate the practical utility of the proposed CP/BTO TENG device, 60 LEDs were connected in series to the device, as shown in Figure 5e. The device CP/BTO successfully powered all 60 LEDs (Supporting Video S1), Additionally, we demonstrated the calculator via a bridge rectifier and capacitor, as illustrated in (Supporting Information Figure S2). The capacitor was connected across the device and the CP/BTO allows the calculator to operate continuously (Supporting Video S2), demonstrating its capacity to operate a low-power electronic device. This demonstration emphasizes the practical utility of the CP/BTO TENG, making it a promising candidate for next-generation high-performance triboelectric nanogenerators suitable for applications in wearable electronics, sensors, and other energy-harvesting technologies.

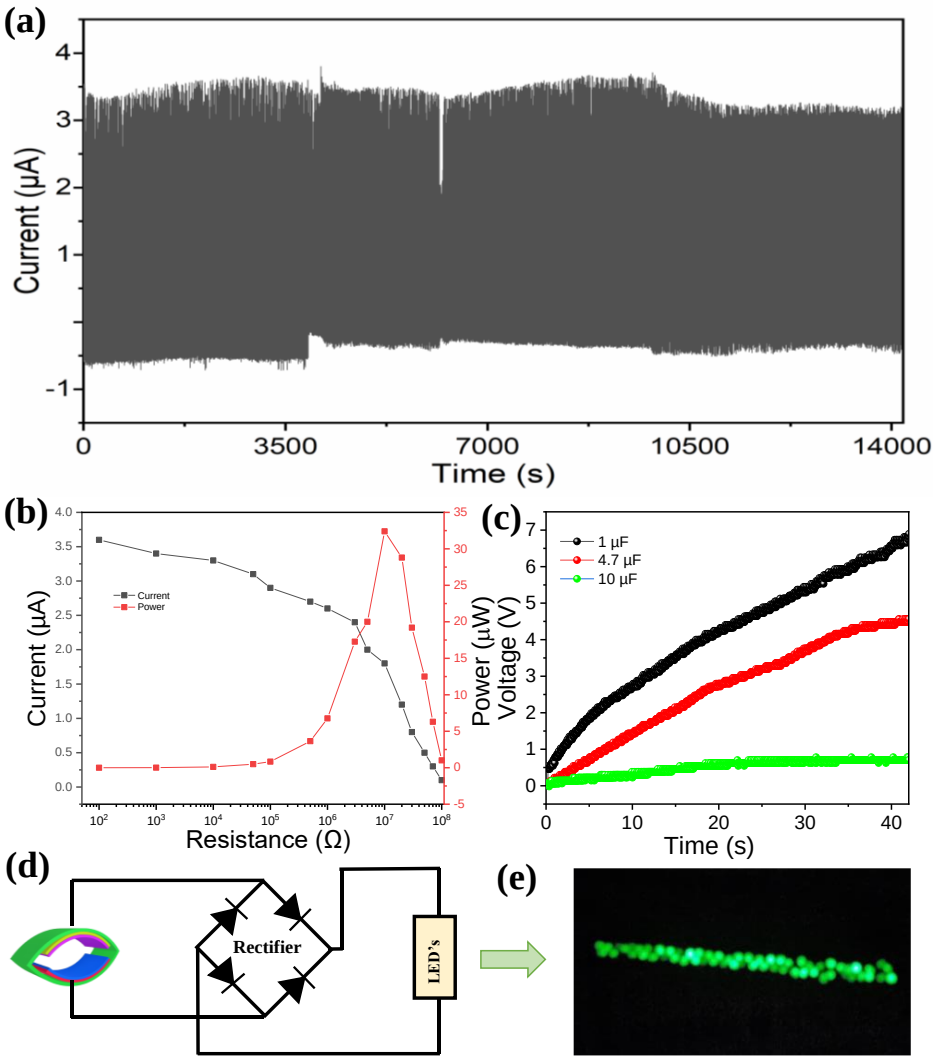


Figure 5. (**a**) Stability of the device at 4 Hz. (**b**) Instantaneous power of CP/BTO device (**c**) capacitor charging of CP/BTO device. (**d**) The electrical schematic showcases the application of LEDs. (**e**) The visual depiction of illuminated LEDs.

4. Conclusions

In this study, we successfully developed a novel triboelectric nanogenerator (TENG) based on copy paper (CP) and barium titanate (BTO) using a screen-printing technique. This approach addresses the limitations of conventional paper-based TENGs by enhancing their energy harvesting capabilities. We systematically investigated the impact of BTO concentration on the device performance, optimizing it from 0% to 20%. The results revealed that 15% BTO concentration yielded the optimal performance, generating a remarkable output of 103 V and 3.6 μA. This represents a significant improvement over the bare copy paper TENG, which produced only 40 V and 1.1 μA. The CP/BTO TENG demonstrated exceptional durability, maintaining stable performance over 57,600 cycles at a frequency of 4 Hz and an applied force of 40 N. This long-term stability is crucial for practical applications in real-world scenarios. We also explored the effects of various parameters on the device's performance. Increasing the applied force from 20 N to 40 N resulted in enhanced output, with the highest performance at 40 N. Similarly, frequency variation from 2 Hz to 4 Hz showed improved output, with 4 Hz yielding the best results before saturation occurred. The device achieved a maximum power density of 32.4 $\mu W/cm^2$, surpassing conventional paper-based TENGs. This high-power density demonstrates the effectiveness of BTO integration in enhancing energy harvesting efficiency. To showcase the practical applicability of our CP/BTO TENG, we successfully powered 60 LEDs and calculator. This demonstration highlights the potential of our device in real-world energy harvesting applications. Furthermore, we investigated the charging capabilities of the device using various capacitors (1 μF, 4.7 μF, and 10 μF), demonstrating its ability to store harvested energy effectively. CP/BTO TENG's performance was also compared using different tribonegative materials (PET and PTFE), with PTFE showing superior results due to its higher tribonegativity.

Supplementary Materials: The following supporting information can be downloaded at: https://www.mdpi.com/article/10.3390/chemosensors13020076/s1, Figure S1: (a) SEM image shows the cross-section of the proposed film. (b) Output voltage of different thickness; Figure S2: (a) The electrical schematic showcasing the application of a calculator. (b) The visual depiction of an illuminated calculator; Figure S3: (a) The realized image of the proposed TENG. (b) Presenting the area of the device as 3×3 cm^2, (c) device in released state, and (d) presenting the area of the device as 3×3 cm^2 in the pressed state; Video S1: LED's lightning for CP/BTO TENG; Video S2: Electronic calculator for CP/BTO TENG.

Author Contributions: Conceptualization, S.L. and O.A.P.; methodology, O.A.P., software, O.A.P. and S.L.; validation, S.L., O.A.P., J.Y.C. and B.L.; investigation, S.L. and O.A.P.; data curation, O.A.P.; writing—original draft preparation, O.A.P., writing—review, and editing, S.L., O.A.P., J.Y.C., B.L. and B.H., supervision, S.L., J.Y.C., B.L. and B.H., funding acquisition, S.L.; All authors have read and agreed to the published version of the manuscript.

Funding: This research was supported by the National University Development Project at Jeonbuk National University in 2024.

Institutional Review Board Statement: Not applicable.

Informed Consent Statement: Not applicable.

Data Availability Statement: The original contributions presented in this study are included in the article/Supplementary Materials. Further inquiries can be directed to the corresponding authors.

Acknowledgments: We thank the funding support from National University Development Project at Jeonbuk National University in 2024.

Conflicts of Interest: The authors declare no conflict of interest.

References

1. Hu, S.; Weber, J.; Chang, S.; Xiao, G.; Lu, J.; Gao, J.; Jiang, W.; Zhang, Y.; Tao, Y. A Low-Cost Simple Sliding Triboelectric Nanogenerator for Harvesting Energy from Human Activities. *Adv. Mater. Technol.* **2022**, *7*, 2200186. [CrossRef]
2. Li, Y.; Zhao, Z.; Gao, Y.; Li, S.; Zhou, L.; Wang, J.; Wang, Z.L. Low-Cost, Environmentally Friendly, and High-Performance Triboelectric Nanogenerator Based on a Common Waste Material. *ACS Appl. Mater. Interfaces* **2021**, *13*, 30776–30784. [CrossRef]
3. Lin, Z.; Zhang, B.; Zou, H.; Wu, Z.; Guo, H.; Zhang, Y.; Yang, J.; Wang, Z.L. Rationally Designed Rotation Triboelectric Nanogenerators with Much Extended Lifetime and Durability. *Nano Energy* **2020**, *68*, 104378. [CrossRef]
4. Chougale, M.Y.; Saqib, Q.M.; Khan, M.U.; Shaukat, R.A.; Kim, J.; Dubal, D.; Bae, J. Expired Pharmaceutical Drugs as Tribopositive Material for Triboelectric Nanogenerator. *Adv. Sustain. Syst.* **2021**, *5*, 2100205. [CrossRef]
5. Xiao, T.X.; Jiang, T.; Zhu, J.X.; Liang, X.; Xu, L.; Shao, J.J.; Zhang, C.L.; Wang, J.; Wang, Z.L. Silicone-Based Triboelectric Nanogenerator for Water Wave Energy Harvesting. *ACS Appl. Mater. Interfaces* **2018**, *10*, 3616–3623. [CrossRef]
6. Jitjaicham, M.; Kusuktham, B. Preparation of Paper Mulberry Fibers and Possibility of Cotton/Paper Mulberry Yarns Production. *Indian J. Mater. Sci.* **2016**, *2016*, 1498967. [CrossRef]
7. He, L.; Zhang, C.; Zhang, B.; Gao, Y.; Yuan, W.; Li, X.; Zhou, L.; Zhao, Z.; Wang, Z.L.; Wang, J. A High-Output Silk-Based Triboelectric Nanogenerator with Durability and Humidity Resistance. *Nano Energy* **2023**, *108*, 108244. [CrossRef]
8. Zhu, Z.; Xia, K.; Xu, Z.; Lou, H.; Zhang, H. Starch Paper-Based Triboelectric Nanogenerator for Human Perspiration Sensing. *Nanoscale Res. Lett.* **2018**, *13*, 365. [CrossRef]
9. Yang, P.K.; Lin, Z.H.; Pradel, K.C.; Lin, L.; Li, X.; Wen, X.; He, J.H.; Wang, Z.L. Paper-Based Origami Triboelectric Nanogenerators and Self-Powered Pressure Sensors. *ACS Nano* **2015**, *9*, 901–907. [CrossRef]
10. Liang, S.; Wang, Y.; Liu, Q.; Yuan, T.; Yao, C. The Recent Progress in Cellulose Paper-Based Triboelectric Nanogenerators. *Adv. Sustain. Syst.* **2021**, *5*, 2100034. [CrossRef]
11. Chi, Y.; Xia, K.; Zhu, Z.; Fu, J.; Zhang, H.; Du, C.; Xu, Z. Rice Paper-Based Biodegradable Triboelectric Nanogenerator. *Microelectron. Eng.* **2019**, *216*, 111059. [CrossRef]
12. Cui, P.; Parida, K.; Lin, M.F.; Xiong, J.; Cai, G.; Lee, P.S. Transparent, Flexible Cellulose Nanofibril–Phosphorene Hybrid Paper as Triboelectric Nanogenerator. *Adv. Mater. Interfaces* **2017**, *4*, 1700651. [CrossRef]
13. Kim, I.; Jeon, H.; Kim, D.; You, J.; Kim, D. All-in-One Cellulose Based Triboelectric Nanogenerator for Electronic Paper Using Simple Filtration Process. *Nano Energy* **2018**, *53*, 975–981. [CrossRef]
14. Wu, W.; Han, S.T.; Venkatesh, S.; Sun, Q.; Peng, H.; Zhou, Y.; Yeung, C.; Li, R.K.Y.; Roy, V.A.L. Biodegradable Skin-Inspired Nonvolatile Resistive Switching Memory Based on Gold Nanoparticles Embedded Alkali Lignin. *Org. Electron.* **2018**, *59*, 382–388. [CrossRef]
15. Choi, D.H.; Kim, H.T.; Kim, Y.; Park, K.; Kim, M.S.; Lee, J.H.; Kim, G.I.; Chung, J.J.; Kim, H.J. Nature-Derived, Biocompatible Silibinin Based Bioresorbable Neuromorphic Device for Implantable Medical Electronics. *Appl. Surf. Sci.* **2023**, *621*, 156814. [CrossRef]
16. Fan, K.; Wei, D.; Zhang, Y.; Wang, P.; Tao, K.; Yang, R. A Whirligig-Inspired Intermittent-Contact Triboelectric Nanogenerator for Efficient Low-Frequency Vibration Energy Harvesting. *Nano Energy* **2021**, *90*, 106576. [CrossRef]
17. Duan, S.; Gao, X.; Wang, Y.; Yang, F.; Chen, M.; Zhang, X.; Ren, X.; Hu, W. Scalable Fabrication of Highly Crystalline Organic Semiconductor Thin Film by Channel-Restricted Screen Printing toward the Low-Cost Fabrication of High-Performance Transistor Arrays. *Adv. Mater.* **2019**, *31*, 1807975. [CrossRef]
18. Hu, S.; Han, J.; Shi, Z.; Chen, K.; Xu, N.; Wang, Y.; Zheng, R.; Tao, Y.; Sun, Q.; Wang, Z.L.; et al. Biodegradable, Super-Strong, and Conductive Cellulose Macrofibers for Fabric-Based Triboelectric Nanogenerator. *Nanomicro Lett.* **2022**, *14*, 115. [CrossRef] [PubMed]
19. Kröger, S.; Turner, A.P.F.; Mosbach, K.; Haupt, K. Imprinted Polymer-Based Sensor System for Herbicides Using Differential-Pulse Voltammetry on Screen-Printed Electrodes. *Anal. Chem.* **1999**, *71*, 3698–3702. [CrossRef] [PubMed]
20. Gao, J.; Miao, L.; Liu, C.; Wang, X.; Peng, Y.; Wei, X.; Zhou, J.; Chen, Y.; Hashimoto, R.; Asaka, T.; et al. A Novel Glass-Fiber-Aided Cold-Press Method for Fabrication of n-Type Ag2Te Nanowires Thermoelectric Film on Flexible Copy-Paper Substrate. *J. Mater. Chem. A Mater.* **2017**, *5*, 24740–24748. [CrossRef]
21. Cao, X.; Chen, H.; Gu, X.; Liu, B.; Wang, W.; Cao, Y.; Wu, F.; Zhou, C. Screen Printing as a Scalable and Low-Cost Approach for Rigid and Flexible Thin-Film Transistors Using Separated Carbon Nanotubes. *ACS Nano* **2014**, *8*, 12769–12776. [CrossRef] [PubMed]
22. Chen, C.; Chen, J.; Han, H.; Chao, L.; Hu, J.; Niu, T.; Dong, H.; Yang, S.; Xia, Y.; Chen, Y.; et al. Perovskite Solar Cells Based on Screen-Printed Thin Films. *Nature* **2022**, *612*, 266–271. [CrossRef] [PubMed]
23. Liu, Z.; Chen, X.; Wang, Z.L. Biopolymer and Biomimetic Techniques for Triboelectric Nanogenerators (TENGs). *Adv. Mater.* **2024**, 2409440. [CrossRef]

24. Ghode, S.B.; Patil, O.A.; Chougale, M.Y.; Nerlekar, N.A.; Patil, S.R.; Patil, C.S.; Pandey Tiwari, A.; Gaikwad, P.K.; Kamat, R.K.; Dandge, P.B.; et al. Terminalia Chebula Fruits Powder as Tribopositive Material for High-Performance Triboelectric Nanogenerator. *Energy Technol.* **2024**, *12*, 2300984. [CrossRef]
25. Pace, G.; del Rio Castillo, A.E.; Lamperti, A.; Lauciello, S.; Bonaccorso, F. 2D Materials-Based Electrochemical Triboelectric Nanogenerators. *Adv. Mater.* **2023**, *35*, 2211037. [CrossRef]
26. Zhang, P.; Zhang, W.; Deng, L.; Zhang, H. A Triboelectric Nanogenerator Based on Temperature-Stable High Dielectric $BaTiO_3$-Based Ceramic Powder for Energy Harvesting. *Nano Energy* **2021**, *87*, 106176. [CrossRef]
27. Zhang, J.H.; Zhang, Y.; Sun, N.; Li, Y.; Du, J.; Zhu, L.; Hao, X. Enhancing Output Performance of Triboelectric Nanogenerator via Large Polarization Difference Effect. *Nano Energy* **2021**, *84*, 105892. [CrossRef]
28. Fatema, M.; Bajpai, A.; Somvanshi, A.; Manzoor, S.; Arshad, M.; Zarrin, N.; Qahtan, A.A.A.; Khan, W.; Husain, S. Study of Structural Correlations with Temperature Dependent Dielectric Response and Ferroelectric Behavior for (Sr, Mn) Co-Doped $BaTiO_3$. *J. Mater. Sci. Mater. Electron.* **2022**, *33*, 6329–6353. [CrossRef]
29. Cho, S.; Yun, C.; Kim, Y.S.; Wang, H.; Jian, J.; Zhang, W.; Huang, J.; Wang, X.; Wang, H.; MacManus-Driscoll, J.L. Strongly Enhanced Dielectric and Energy Storage Properties in Lead-Free Perovskite Titanate Thin Films by Alloying. *Nano Energy* **2018**, *45*, 398–406. [CrossRef]
30. Pant, H.C.; Patra, M.K.; Verma, A.; Vadera, S.R.; Kumar, N. Study of the Dielectric Properties of Barium Titanate-Polymer Composites. *Acta Mater.* **2006**, *54*, 3163–3169. [CrossRef]
31. Kim, J.Y.; Lee, J.W.; Jung, H.S.; Shin, H.; Park, N.G. High-Efficiency Perovskite Solar Cells. *Chem. Rev.* **2020**, *120*, 7867–7918. [CrossRef] [PubMed]
32. Wu, Y.; Wei, Y.; Huang, Y.; Cao, F.; Yu, D.; Li, X.; Zeng, H. Capping CsPbBr3 with ZnO to Improve Performance and Stability of Perovskite Memristors. *Nano Res.* **2017**, *10*, 1584–1594. [CrossRef]
33. Sahu, M.; Hajra, S.; Bijelic, J.; Oh, D.; Djerdj, I.; Kim, H.J. Triple Perovskite-Based Triboelectric Nanogenerator: A Facile Method of Energy Harvesting and Self-Powered Information Generator. *Mater. Today Energy* **2021**, *20*, 100639. [CrossRef]
34. Hatta, F.F.; Mohammad Haniff, M.A.S.; Ambri Mohamed, M. Enhanced-Performance Triboelectric Nanogenerator Based on Polydimethylsiloxane/Barium Titanate/Graphene Quantum Dot Nanocomposites for Energy Harvesting. *ACS Omega* **2024**, *9*, 5608–5615. [CrossRef] [PubMed]
35. Wang, J.; Wu, H.; Wang, Z.; He, W.; Shan, C.; Fu, S.; Du, Y.; Liu, H.; Hu, C. An Ultrafast Self-Polarization Effect in Barium Titanate Filled Poly(Vinylidene Fluoride) Composite Film Enabled by Self-Charge Excitation Triboelectric Nanogenerator. *Adv. Funct. Mater.* **2022**, *32*, 2204322. [CrossRef]
36. Yu, J.; Hou, X.; Cui, M.; Zhang, N.; Zhang, S.; He, J.; Chou, X. Skin-Conformal BaTiO3/Ecoflex-Based Piezoelectric Nanogenerator for Self-Powered Human Motion Monitoring. *Mater. Lett.* **2020**, *269*, 127686. [CrossRef]
37. Min, G.; Pullanchiyodan, A.; Dahiya, A.S.; Hosseini, E.S.; Xu, Y.; Mulvihill, D.M.; Dahiya, R. Ferroelectric-Assisted High-Performance Triboelectric Nanogenerators Based on Electrospun P(VDF-TrFE) Composite Nanofibers with Barium Titanate Nanofillers. *Nano Energy* **2021**, *90*, 106600. [CrossRef]
38. Hajra, S.; Padhan, A.M.; Sahu, M.; Alagarsamy, P.; Lee, K.; Kim, H.J. Lead-Free Flexible Bismuth Titanate-PDMS Composites: A Multifunctional Colossal Dielectric Material for Hybrid Piezo-Triboelectric Nanogenerator to Sustainably Power Portable Electronics. *Nano Energy* **2021**, *89*, 106316. [CrossRef]
39. Pawar, O.Y.; Ha, H.; Qaiser, N.; Kim, S.H.; Hwang, B.; Lim, S. The Effect of Printing Parameters on the Bonding Strength and Electric Performance of FDM-Printed Graphene Filaments to Mulberry Paper for Paper Electronics. *Cellulose* **2024**, *31*, 1741–1754. [CrossRef]
40. Tang, Q.; Guo, H.; Yan, P.; Hu, C. Recent Progresses on Paper-Based Triboelectric Nanogenerator for Portable Self-Powered Sensing Systems. *EcoMat* **2020**, *2*, e12060. [CrossRef]
41. Lacks, D.J.; Shinbrot, T. Long-Standing and Unresolved Issues in Triboelectric Charging. *Nat. Rev. Chem.* **2019**, *3*, 465–476. [CrossRef]
42. Verners, O.; Lapčinskis, L.; Sherrell, P.C.; Šutka, A. Contact Electrification at Dielectric Polymer Interfaces: On Bond Scission, Material Transfer, and Electron Transfer. *Adv. Mater. Interfaces* **2023**, *10*, 2300562. [CrossRef]
43. Hao, S.; Fu, D.; Li, J.; Wang, W.; Shen, B. Preparation and Characterization of Ag-Doped BaTiO 3 Conductive Powders. *Int. J. Inorg. Chem.* **2011**, *2011*, 837091. [CrossRef]
44. Qian, C.; Li, L.; Gao, M.; Yang, H.; Cai, Z.; Chen, B.; Xiang, Z.; Zhang, Z.; Song, Y. Nano Energy All-Printed 3D Hierarchically Structured Cellulose Aerogel Based Triboelectric Nanogenerator for Multi-Functional Sensors. *Nano Energy* **2019**, *63*, 103885. [CrossRef]
45. Chen, X.; Xiong, J.; Parida, K.; Guo, M.; Wang, C.; Wang, C.; Li, X.; Shao, J.; Lee, P.S. Transparent and Stretchable Bimodal Triboelectric Nanogenerators with Hierarchical Micro-Nanostructures for Mechanical and Water Energy Harvesting. *Nano Energy* **2019**, *64*, 103904. [CrossRef]

46. Guo, Q.Z.; Liu, C.P. Derivation of Analytical Equations with Experimental Verification for Working Mechanism of Triboelectric Nanogenerators in Contact-Separation Mode. *Nano Energy* **2020**, *76*, 104969. [CrossRef]
47. Tabassian, R.; Rajabi-Abhari, A.; Mahato, M.; Yoo, H.; Yoon, H.Y.; Park, J.Y.; Oh, I.K. Metal-Organic Framework-Based Nanofibrous Film for Two Different Modes of Triboelectric Nanogenerators. *SmartMat* **2024**, *5*, e1270. [CrossRef]
48. Zi, Y.; Wu, C.; Ding, W.; Wang, Z.L. Maximized Effective Energy Output of Contact-Separation-Triggered Triboelectric Nanogenerators as Limited by Air Breakdown. *Adv. Funct. Mater.* **2017**, *27*, 1700049. [CrossRef]

Disclaimer/Publisher's Note: The statements, opinions and data contained in all publications are solely those of the individual author(s) and contributor(s) and not of MDPI and/or the editor(s). MDPI and/or the editor(s) disclaim responsibility for any injury to people or property resulting from any ideas, methods, instructions or products referred to in the content.